

Extension of the energy range of experimental activation cross-sections data of deuteron induced nuclear reactions on indium up to 50 MeV

F. Tárkányi^a, F. Ditrói^{a,*}, S. Takács^a, A. Hermanne^b, A.V. Ignatyuk^c

^a*Institute for Nuclear Research, Hungarian Academy of Sciences (ATOMKI), Debrecen, Hungary*

^b*Cyclotron Laboratory, Vrije Universiteit Brussel (VUB), Brussels, Belgium*

^c*Institute of Physics and Power Engineering (IPPE), Obninsk, Russia*

Abstract

The energy range of our earlier measured activation cross-sections data of longer-lived products of deuteron induced nuclear reactions on indium were extended from 40 MeV up to 50 MeV. The traditional stacked foil irradiation technique and non-destructive gamma spectrometry were used. No experimental data were found in literature for this higher energy range. Experimental cross-sections for the formation of the radionuclides $^{113,110}\text{Sn}$, $^{116m,115m,114m,113m,111,110g,109}\text{In}$ and ^{115}Cd are reported in the 37-50 MeV energy range, for production of ^{110}Sn and $^{110g,109}\text{In}$ these are the first measurements ever. The experimental data were compared with the results of cross section calculations of the ALICE and EMPIRE nuclear model codes and of the TALYS1.6 nuclear model code as listed in the on-line library TENDL-2014.

Keywords: indium target, deuteron activation, Sn, In and Cd radioisotopes

1. Introduction

In the frame of our systematic study of charged particle induced activation, we earlier investigated the activation cross sections induced by deuterons on natural indium targets (Tárkányi et al., 2011). The main aim was then to study the production possibility of the $^{113/113m}\text{In}$ medical generator up to the available 40 MeV deuteron energy at the CYRIC (Tohoku University) AVF cyclotron. The activation cross sections on indium are however of importance not only for the mentioned generator, but four other medically relevant radionuclides can be produced: ^{114m}In (49.51 d), ^{113m}In (99.476 min), ^{111}In (2.8047 d) and ^{110m}In (69.1 min). For the last three, apart from direct reactions also decay from parent ^{113}Sn (115.09 d), ^{111}Sn (35.3 min) and ^{110}Sn (4.11 h) is contributing. Taking into account that no earlier data are available above 40 MeV incident deuteron energy and having the possibility to irradiate in the 50 MeV beam of the LLN Cyclone 90 cyclotron, we decided to extend the energy range of our previous study. Similar investigation is in progress on cross sections of proton induced reactions on indium up to 70

MeV by using different accelerators. The possible applications of the experimental data are discussed in our 2011 publication. Here we summarize the new experimental results, including only a short summary of the specific characteristics of experimental technique and the data evaluation method. The theoretical results calculated with ALICE-D code (Dityuk et al., 1998) and the EMPIRE-D code (Herman et al., 2007) were taken from the previous work, while for the calculation with the Talys code (Koning et al., 2007) the latest data available in the TENDL-2014 library (Koning and Rochman, 2013), based on the TALYS 1.6 version were used.

2. Experiment and data evaluation

For the cross section determination an activation method based on stacked foil irradiation technique and followed by γ -ray spectrometry were used. In order to avoid contamination of the stack by indium or its activation products in the case of accidental overheating, the In targets consisted of sandwiches of thin In foils backed by 50 μm Al and covered by a thin (6 μm) Al foil. The stack bombarded for 3600 s with a 50 MeV deuteron beam of 32 nA at Louvain la Neuve consisted of a sequence of Rh, Al, Al-In-Al, Pd, Al, Nb, Al foils (thicknesses are in Table 1) repeated 9 times.

*Corresponding author: ditroi@atomki.hu

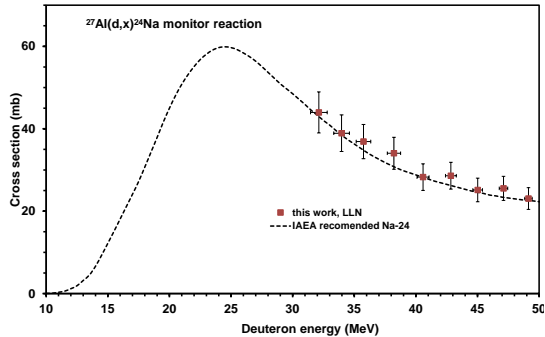


Figure 1: Monitor reaction for $^{27}\text{Al}(d,x)^{24}\text{Na}$ nuclear reaction

The deuteron beam was degraded from 50 MeV down to 32 MeV in the last In foil of the stack, assuring a good energy overlap with the 2011 study. Additional details on experiment, on beam parameters and on the data evaluation can be found in our earlier works made at same accelerator by using the same technique (Hermann et al., 2014). The main experimental parameters and the methods of data evaluation for the present study are summarized in Table 1. The used decay data are collected in Table 2. The experimental data were measured relative to the $^{27}\text{Al}(d,x)^{24}\text{Na}$ monitor reaction (see Fig. 1). The uncertainty of the experimental points was estimated by the common technique according to the ISO guide (International-Bureau-of-Weights-and-Measures, 1993). The calculated experimental uncertainties are as follows: number of target nuclei including non-uniformity (5 %), incident deuteron flux (7 %), peak area including statistical errors of counts (0.1-20 %), detector efficiency (5 %), γ -ray abundance and branching ratio (3 %). Except for a few data points the total uncertainty of 10-15 % was obtained as positive square root of the quadratic sum of the individual uncertainty sources. Possible additional uncertainties due to non-linear effects of half-lives and cooling time were not taken into account.

3. Cross sections

The measured cross sections for the production of $^{113,110}\text{Sn}$, $^{116m,115m,114m,113m,111,110g,109}\text{In}$ and ^{115}Cd are shown in Table 3 and Figures 2-11. The figures also show the theoretical results calculated with the ALICE-IPPE-D and the EMPIRE-D codes and the values avail-

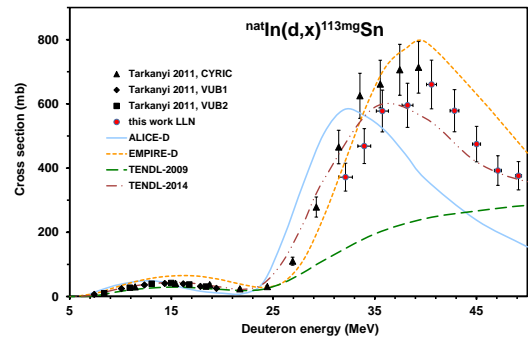


Figure 2: Experimental and theoretical cross sections for the formation of ^{113}Sn by the deuteron bombardment of indium

able in the TALYS based TENDL-2014 library. The results for ^{115g}Cd are significantly different compared what was published in our earlier work in the overlapping energy range. After a detailed check of both data evaluations an input mistake was discovered in the calculation sheet (the detector efficiency) of the earlier work. The results were corrected and are shown in Fig. 11. In most of the other excitation function a slight systematic shift can be observed, which could be caused by the different spectrometer system (efficiency calibration) and by the fact that all of our measurements are relative measurements to the monitor reactions. An improvement in the monitor reaction data can result in a modified excitation function by the nuclear reactions in question. The theoretical model calculations are taken from our previous work (except TENDL-2014 and for ^{110}Sn , ^{110g}In and ^{109}In isotopes), which are new, compared to our previous work.

3.1. ^{113}Sn

The excitation function of ^{113}Sn (Fig. 2) was measured after total decay of the short-lived meta-stable state (21.4 min, IT 91 %) to the long-lived ground state (115.1 d). An acceptable agreement with our earlier measurements can be seen. Clear improvement of description by the TALYS code in the new TENDL data can be observed.

3.2. ^{110}Sn

The experimental excitation functions for production of ^{110}Sn (4.11 h) are shown in Fig. 3 in comparison with the TENDL-2014 predictions. Because it is a new

Table 1: Main parameters of the experiment and the methods of data evaluations

Experiment		Data evaluation	
Incident particle	Deuteron	Gamma spectra evaluation	Genie 2000, (Canberra, 2000), Forgamma (Székely, 1985)
Method	Stacked foil	Determination of beam intensity	Faraday cup (preliminary)/Fitted monitor reaction (final)(Tárkányi et al., 1991)
Target stack and thicknesses	Rh (26 μm), Al(50 μm), Al(6 μm)-In(50 μm)-Al(50 μm), Pd(8 μm), Al(50 μm), Nb(10 μm), Al(50 μm) block Repeated 9 times	Decay data	NUDAT 2.6 (NuDat, 2014)
Number of target foils	9x7	Reaction Q-values	Q-value calculator (Pritychenko and Sonzogni, 2003)
Accelerator	Cyclone 90 cyclotron of the Université Catholique in Louvain la Neuve (LLN) Belgium	Determination of beam energy	(Andersen and Ziegler, 1977) (preliminary)/Fitted monitor reaction (final) (International-Bureau-of-Weights-and-Measures, 1993; Tárkányi et al., 2001)
Primary energy	50 MeV	Uncertainty of energy	Cumulative effects of possible uncertainties
Irradiation time	60 min	Cross sections	Isotopic cross section
Beam current	32 nA	Uncertainty of cross sections	Sum in quadrature of all individual contribution
Monitor reaction, [recommended values]	$^{27}\text{Al}(d,x)^{24}\text{Na}$ reaction	Yield	Physical yield (Bonardi, 1987)
Monitor target and thickness	^{27}Al 50+6 μm	Theory	ALICE-IPPE (Dityuk et al., 1998), ALICE-IPPE-D (Ignatyuk, 2010) EMPIRE (Herman et al., 2007); EMPIRE-D (Ignatyuk, 2011); TALYS (Koning and Rochman, 2013; Koning et al., 2014)
detector	HPGe		
γ -spectra measurements	4 series		
Cooling times (h)	6.5-8.2 45.2-49.8 116.2-125.0 557-582		

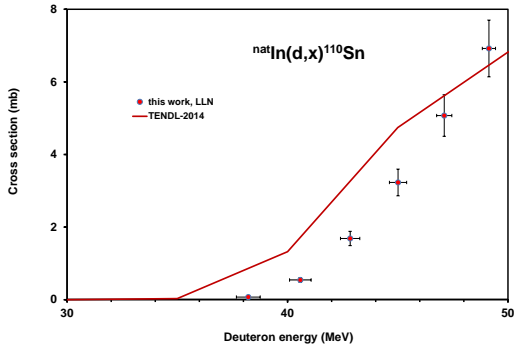


Figure 3: Experimental and theoretical cross sections for the formation of ^{110}Sn by the deuteron bombardment of indium

series of data compared to or previous work in the same topic (Tárkányi et al., 2011), only the new TENDL-2014 predictions were re-calculated. No earlier experimental data exist.

3.3. $^{116m1}\text{In}(m2+)$

The cross sections of the first metastable state (54.29 min) were measured after complete decay of the second metastable state (2.18 s), which decays to m1 by 100 % IT (Fig. 4). An acceptable agreement with our earlier measurements has been observed. No real change in description by TALYS code was done. All theoretical model calculations underestimate the experimental values except ALICE-D above 35 MeV.

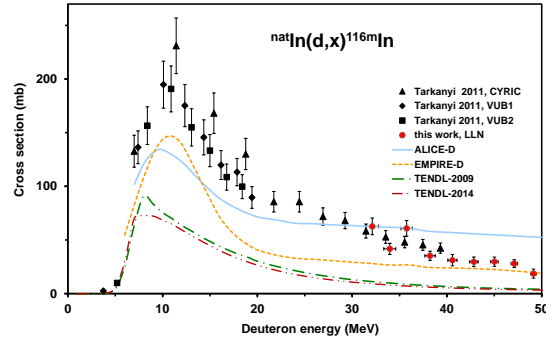


Figure 4: Experimental and theoretical cross sections for the formation of $^{116m1}\text{In}(m2+)$ by the deuteron bombardment of indium

Table 2: Decay data of the investigated reaction products (NuDat, 2014; Pritychenko and Sonzogni, 2003)

Nuclide	Half-life	Decay method	E_γ (keV)	I_γ (%)	Contributing reaction	Q-value(keV)
^{113m}Sn 7/2 ⁺ 77.382	21.4 min	EC 8.9 IT 91.1	77	0.501	$^{113}\text{In}(d,2n)$ $^{115}\text{In}(d,4n)$	-4044.5 -20357.66
^{113g}Sn 7/2 ⁺	115.09 d	EC 100	255.134 391.698	2.11 64.97	$^{113}\text{In}(d,2n)$ $^{115}\text{In}(d,4n)$	-4044.5 -20357.66
^{111}Sn 7/2 ⁺	35.3 min	EC 69.8 β^+ 30.25	372.31 761.97 954.05 1152.98 1610.47	0.42 1.48 0.51 2.7 1.31	$^{113}\text{In}(d,4n)$ $^{115}\text{In}(d,6n)$	-22575.87 -38889.03
^{110}Sn 0 ⁺	4.11 h	EC 100	280.462	100	$^{113}\text{In}(d,5n)$ $^{115}\text{In}(d,7n)$	-30744.7 -47057.9
^{109}Sn 5/2 ⁺	18 min	EC 93.6 β^+ 6.6	649.8 1099.2 1321.3	28 30 11.9	$^{113}\text{In}(d,6n)$ $^{115}(d,8n)$	-42027.11 -58340.26
$^{116m1}\text{In}$ 5 ⁺ 127.267	54.29 min	β^- 100	1097.3	56.2	$^{115}\text{In}(d,p)$ decay of $^{116m2}\text{In}$	4560.154
^{115m}In 1/2 ⁻ 336.24417	4.486 h	IT: 95.0 β^- : 5.0	336.24	45.8	$^{115}\text{In}(d,pn)$	-2224.566
^{114m}In 5 ⁺ 190.3682	49.51 d	EC 3.25 IT 96.75	190.27 558.43 725.24	15.56 3.2 3.2	$^{113}\text{In}(d,p)$ $^{115}\text{In}(d,p2n)$	5049.324 -11263.836
^{113m}In 1/2 ⁻ 391.691	99.476 min	IT 100	391.698	64.94	$^{113}\text{In}(d,pn)$ $^{115}\text{In}(d,p3n)$	-2224.566 -18537.734
^{111}In 9/2 ⁺	2.8047 d	ϵ : 100	171.28 245.35	90.7 94.1	$^{113}\text{In}(d,p3n)$ $^{115}\text{In}(d,p5n)$ decay of ^{111m}In and ^{111}Sn	-19342.13 -35655.3
^{110m}In 2 ⁺ 62.08	69.1 min	β^+ 61.3 EC 38.7	657.75	97.74	$^{113}\text{In}(d,p4n)$ $^{115}\text{In}(d,p6n)$ ^{110}Sn decay	-29333.6 -45646.7
^{110g}In 7 ⁺	4.92 h	β^+ 0.0081 EC 99.9919	641.68 657.75 707.40 937.478 997.16	26 98 29.5 68.4 10.5	$^{113}\text{In}(d,p4n)$ $^{115}\text{In}(d,p6n)$	-29333.6 -45646.7
^{109}In	4.167 h	EC 95.44 β^+ 4.56	203.5 426.2 623.5	73.5 4.12 5.5	$^{113}\text{In}(d,p5n)$ $^{115}\text{In}(d,p7n)$	-37387.74 -53700.9
^{115g}Cd 1/2 ⁺	53.46 h	β^- 100	581.87 1109.76	33.1 62.6	$^{115}\text{In}(d,2p)$	-2894.172

Abundances in ^{nat}In : ^{113}In 4.29 %, ^{115}In 95.71 %. In case of clustered emission change the Q values by: pn→d: +2.2 MeV, p2n→t: +8.5 MeV

3.4. ^{115m}In

The ^{115m}In metastable state (4.486 h) can be produced directly via the $^{115}\text{In}(d,pn)$ reaction and through decay of ^{115}Cd . No gamma-lines from the decay of significantly longer-lived isomers of ^{115}Cd were detected in the spectra measured shortly after EOB, indicating the negligible contribution to the ^{115m}In production. The cross sections therefore can hence be considered as direct independent production cross sections (Fig. 5). An acceptable agreement with our earlier measurements is seen. The description by the recent version of the TALYS code is better than before.

3.5. ^{114m}In

The independent cross sections for formation of the metastable state of the ^{114}In ($T_{1/2} = 49.51$ d) are shown in Fig. 6. The contribution of reactions on both stable indium isotopes can be distinguished. Our new results connect well to the earlier measurements, but give lower values in the overlapping energy range The description

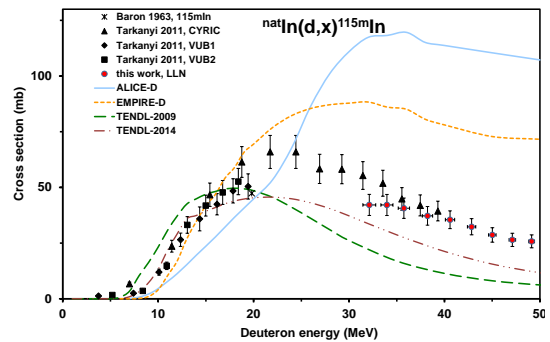


Figure 5: Experimental and theoretical cross sections for the formation of ^{115m}In by the deuteron bombardment of indium

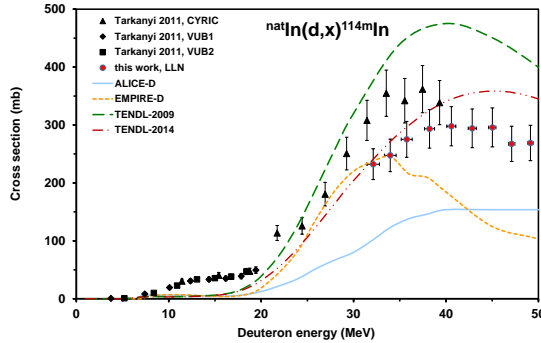


Figure 6: Experimental and theoretical cross sections for the formation of ^{114m}In by the deuteron bombardment of indium

of the $^{113}\text{In}(d,p)^{114m}\text{In}$ reaction is not improved in the newest version of the TALYS code.

3.6. ^{113m}In

The ^{113m}In (99.476 min) can be produced directly via (d,pxn) reaction and through decay of long-lived ^{113g}Sn (115.09 d). Based on the measured ^{113}Sn cross section (see above), no significant contribution of parent decay was estimated in the first gamma spectra used for calculation of ^{113m}In production cross sections (Fig. 7). Good agreement with our earlier measurement and slight improvement of the description by the TALYS code were observed.

3.7. ^{111}In

The measured cross sections (Fig. 8) of ^{111g}In (2.8047 d) are cumulative, including also production through isomeric transition of the short-lived ^{111m}In metastable state (7.7 min) and decay of ^{111}Sn parent (35.3 min). An acceptable agreement with our earlier measurements and clear improvement of the TALYS description above 25 MeV were observed.

3.8. ^{110g}In

The independent cross sections for production of ^{110g}In (4.92 h) are shown in Fig. 9. No earlier experimental data were found. The description by TENDL-2014 is acceptable good, the other theoretical model codes are not used in this case.

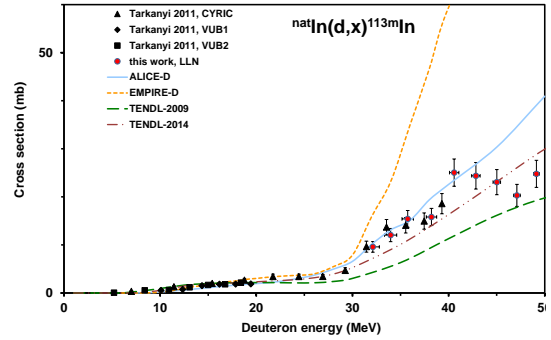


Figure 7: Experimental and theoretical cross sections for the formation of ^{113m}In by the deuteron bombardment of indium

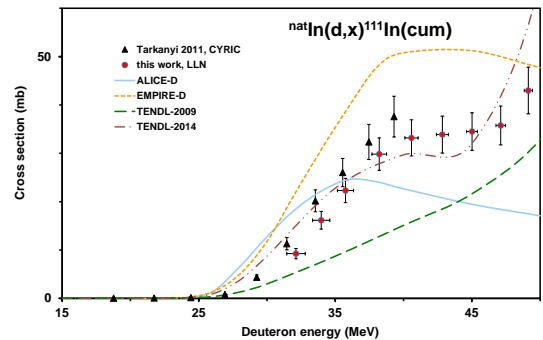


Figure 8: Experimental and theoretical cross sections for the formation of ^{111}In by the deuteron bombardment of indium

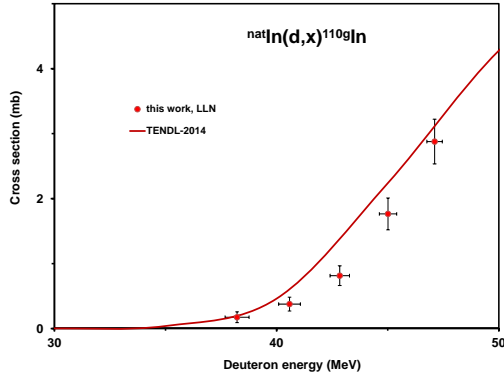


Figure 9: Experimental and theoretical cross sections for the formation of ^{110g}In by the deuteron bombardment of indium

3.9. ^{109}In

We obtained cross sections for ^{109}In (4.167 h) only at two high energy points (Fig. 10). No earlier data were found in the literature. The only theoretical model calculation with TENDL-2014 overestimates the experimental values.

3.10. ^{115g}Cd

The new independent cross section data for the $^{nat}\text{In}(d,x)^{115g}\text{Cd}$ process is shown in Fig. 11, together with the published and corrected data of (Tárkányi et al., 2011) (see explanation of needed correction earlier) A good agreement exist between the two datasets. All codes give results that are about one order of magnitude off the experimental values.

4. Summary and conclusion

We report experimental cross sections for production of $^{113,110}\text{Sn}$, $^{116m,115m,114m,113m,111,110g,109}\text{In}$ and ^{115}Cd in the 37-50 MeV energy range. The new data are first data sets for all products above 40 MeV and for production of ^{110}Sn and $^{110g,109}\text{In}$ no earlier experimental data were found. The experimental and theoretical data and the deduced integral yields were compared in detail in our 2011 publication. The comparison between the 2009 and 2014 versions of the TENDL library (obtained with the most recent version of the TALYS codes) shows further improvement for (d,xn) and some (d,pxn) reactions but the agreement is still poor when the (d,p) reactions plays an important role. The possible use of experimental data for production was discussed in detail in our

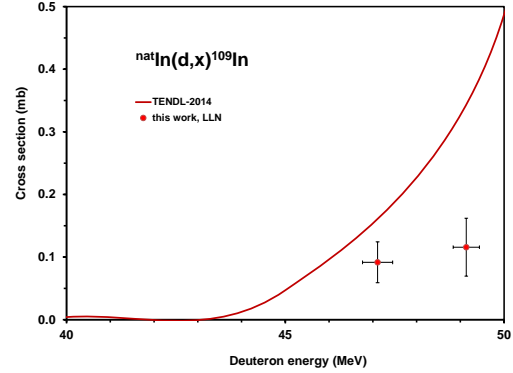


Figure 10: Experimental and theoretical cross sections for the formation of ^{109}In by the deuteron bombardment of indium

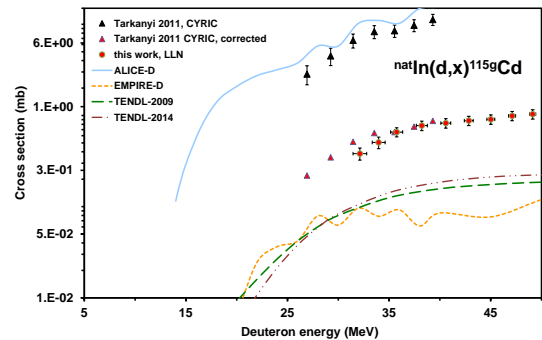


Figure 11: Experimental and theoretical cross sections for the formation of ^{115m}Cd by the deuteron bombardment of indium

Table 3: Measured experimental data points for the $^{nat}\text{In}(p,x)^{113,110}\text{Sn}$, $^{116m,115m,114m,113m,111,110g,109}\text{In}$, ^{115}Cd nuclear reactions

Energy (MeV)		Cross section (mb)																			
E	ΔE	^{113m}Sn		^{110}Sn		^{116m}In		^{115m}In		^{114m}In		^{113m}In		^{111}In		^{110g}In		^{109}In		^{115g}Cd	
		σ	$\pm\Delta\sigma$	σ	$\pm\Delta\sigma$	σ	$\pm\Delta\sigma$	σ	$\pm\Delta\sigma$	σ	$\pm\Delta\sigma$	σ	$\pm\Delta\sigma$	σ	$\pm\Delta\sigma$	σ	$\pm\Delta\sigma$	σ	$\pm\Delta\sigma$	σ	$\pm\Delta\sigma$
49.14	0.30	376.0	44.1	6.9	0.8	18.7	4.2	25.8	2.9	269.0	30.6	24.8	2.8	43.0	4.8	4.1	0.5	0.12	0.05	1.03	0.12
47.11	0.34	392.3	46.1	5.1	0.6	28.1	3.5	26.5	3.0	267.5	30.5	20.3	2.3	35.8	4.0	2.9	0.3	0.09	0.03	0.99	0.12
45.01	0.39	474.7	55.3	3.2	0.4	29.9	4.3	28.7	3.2	295.8	33.6	23.1	2.6	34.5	3.9	1.8	0.2			0.91	0.11
42.84	0.44	578.6	65.6	1.7	0.2	29.8	4.5	32.3	3.6	294.3	33.5	24.4	2.8	33.9	3.8	0.81	0.15			0.88	0.10
40.58	0.49	660.4	75.8	0.54	0.07	31.2	5.2	35.5	4.0	297.8	33.9	25.0	2.8	33.2	3.7	0.38	0.11			0.82	0.10
38.22	0.54	595.6	68.7	0.07	0.03	35.3	4.3	37.2	4.2	293.4	33.4	15.8	1.8	29.8	3.4	0.17	0.08			0.77	0.09
35.75	0.59	577.8	65.3			60.9	7.3	40.7	4.6	275.2	31.0	15.4	1.7	22.3	2.5					0.66	0.08
33.97	0.63	468.5	54.4			41.8	5.2	42.1	4.7	247.6	28.2	12.1	1.4	16.2	1.8					0.51	0.07
32.12	0.67	371.7	43.4			62.8	7.8	42.1	4.7	232.4	26.6	9.6	1.1	9.2	1.1					0.38	0.06

previous work and for ^{110m}In , ^{111}In , ^{113m}In and ^{114m}In will be included in our simultaneously submitted work on proton induced nuclear reactions on indium. The direct productions of indium radionuclides on indium target will in all cases be carrier added. Therefore for production of these medical radioisotopes via deuteron induced reactions on indium only the production possibility through generator parent isotopes should be taken into account.

5. Acknowledgements

This work was performed in the frame of the HAS-FWO Vlaanderen (Hungary-Belgium) project. The authors acknowledge the support of the research project and of the respective institutions. We thank to Cyclotron Laboratory of the Université Catholique in Louvain la Neuve (LLN) providing the beam time and the crew of the LLN Cyclone 90 cyclotron for performing the irradiations.

References

Andersen, H. H., Ziegler, J. F., 1977. Hydrogen stopping powers and ranges in all elements. The stopping and ranges of ions in matter, Volume 3. The Stopping and ranges of ions in matter. Pergamon Press, New York.

Bonardi, M., 1987. The contribution to nuclear data for biomedical radioisotope production from the milan cyclotron facility. Canberra, 2000. http://www.canberra.com/products/radiochemistry_lab/genie-2000-software.asp.

Dityuk, A. I., Konobeyev, A. Y., Lunev, V. P., Shubin, Y. N., 1998. New version of the advanced computer code alice-ippe. Tech. rep., IAEA.

Herman, M., Capote, R., Carlson, B. V., Oblozinsky, P., Sin, M., Trkov, A., Wienke, H., Zerkin, V., 2007. Empire: Nuclear reaction model code system for data evaluation. Nuclear Data Sheets 108 (12), 2655–2715.

Hermanne, A., Tárkányi, F., Takács, S., 2014. Activation cross sections for production of ^7Be by proton and deuteron induced reactions on ^9Be : Protons up to 65 mev and deuterons up to 50 mev. Applied Radiation and Isotopes 90 (0), 203–207.

Ignatyuk, A. V., 2010. 2nd rcm on fendl-3 http://www-nds.iaea.org/fendl3/rcm2_slides.html.

Ignatyuk, A. V., 2011. Phenomenological systematics of the (d,p) cross sections, http://www-nds.iaea.org/fendl3/000pages/rcm3/slides/ignatyuk_fendl-3

International-Bureau-of-Weights-and-Measures, 1993. Guide to the expression of uncertainty in measurement, 1st Edition. International Organization for Standardization, Genève, Switzerland.

Koning, A. J., Hilaire, S., Duijvestijn, M. C., 2007. Talys-1.0.

Koning, A. J., Rochman, D., 2013. Talys-based evaluated nuclear data library.

Koning, A. J., Rochman, D., van der Marck, S., Kopecky, J., Sublet, J. C., Pomp, S., Sjostrand, H., Forrest, R., Bauge, E., Henriksson, H., Cabellos, O., Goriely, S., Leppanen, J., Leeb, H., Plompen, A., Mills, R., 2014. Tendl-2014: Talys-based evaluated nuclear data library.

NuDat, 2014. Nudat2 database (2.6).

Pritychenko, B., Sonzogni, A., 2003. Q-value calculator.

Székely, G., 1985. Fgm - a flexible gamma-spectrum analysis program for a small computer. Computer Physics Communications 34 (3), 313–324.

Tárkányi, F., Hermanne, A., Király, B., Takács, S., Ditrói, F., Baba, M., Ignatyuk, A. V., 2011. Investigation of activation cross sections of deuteron induced reactions on indium up to 40 mev for production of a $^{113}\text{In}/^{113m}\text{In}$ generator. Applied Radiation and Isotopes 69 (1), 26–36.

Tárkányi, F., Szelecsényi, F., Takács, S., 1991. Determination of effective bombarding energies and fluxes using improved stacked-foil technique. Acta Radiologica, Supplementum 376, 72.

Tárkányi, F., Takács, S., Gul, K., Hermanne, A., Mustafa, M. G., Nortier, M., Oblozinsky, P., Qaim, S. M., Scholten, B., Shubin, Y. N., Youxiang, Z., 2001. Charged particles cross-sections database for medical radioisotope production, beam monitors reactions.